Concurrent targeting of MAP3K3 and BRD4 by *miR-3140-3p* overcomes acquired resistance to BET inhibitors in neuroblastoma cells

Chang Liu,[1] Yasuyuki Gen,[1] Kousuke Tanimoto,[2] Tomoki Muramatsu,[1] Jun Inoue,[1] and Johji Inazawa[1,3]

[1]Department of Molecular Cytogenetics, Medical Research Institute, Tokyo Medical and Dental University (TMDU), 1-5-45 Yushima, Bunkyo-ku, Tokyo 113-8510, Japan; [2]Genome Laboratory, Medical Research Institute, TMDU, Tokyo, Japan; [3]Bioresource Research Center, Tokyo Medical and Dental University, Bunkyo-ku, Tokyo, Japan

Neuroblastoma (NB) harboring *MYCN* amplification is a refractory disease with a poor prognosis. As BRD4, an epigenetic reader belonging to the bromodomain and extra terminal domain (BET) family, drives transcription of *MYCN* in NB cells, BET inhibitors (BETis) are considered useful for NB therapy. However, clinical trials of BETis suggested that early acquired resistance to BETis limits their therapeutic benefit. MicroRNAs are small non-coding RNAs that mediate post-transcriptional silencing of target genes. We previously identified *miR-3140-3p* as a potent candidate for nucleic acid therapeutics for cancer, which directly targets *BRD4*. We demonstrated that *miR-3140-3p* suppresses tumor cell growth in *MYCN*-amplified NB by downregulating MYCN and MYC through BRD4 suppression. We established BETi-acquired resistant NB cells to evaluate the mechanism of resistance to BETi in NB cells. We revealed that activated ERK1/2 stabilizes MYCN protein by preventing ubiquitin-mediated proteolysis via phosphorylation of MYCN at Ser62 in BETi-acquired resistant NB cells, thereby attenuating the effects of BETi in these cells. *miR-3140-3p* efficiently downregulated MYCN expression by directly targeting the MAP3K3-ERK1/2 pathway in addition to BRD4 suppression, inhibiting tumor cell growth in BETi-acquired resistant NB cells. This study suggests that *miR-3140-3p* has the potential to overcome resistance to BETi in NB.

INTRODUCTION

Neuroblastoma (NB), which originates from undifferentiated neural crest cells, is the most common pediatric extracranial solid tumor.[1] According to the International Neuroblastoma Risk Group classification, the pretreatment risk of NB is classified as very low, low, intermediate, or high.[2] The prognosis is favorable for NB in very low- and low-risk groups, whereas NB in the high-risk group is generally refractory with a poor prognosis despite comprehensive therapy, including surgery, chemotherapy, radiotherapy, and immunotherapy.[3,4] Thus, novel therapeutic approaches are needed for high-risk NB tumors.

MYCN, a highly homologous member of the *MYC* oncogenes, is amplified in ~50% of high-risk NB.[5] Functionally, MYCN regulates the transcriptional program similar to MYC, playing an essential role in the growth of NB cells.[6,7] Therefore, MYCN is not only a prognostic marker but also a therapeutic target of NB. BRD4, an epigenetic reader belonging to the bromodomain and extra terminal domain (BET) family, drives transcription of oncogenes, including *MYC,* in cancer cells.[8] Recent studies revealed that BRD4 binds to super-enhancers of *MYCN* to drive its transcription in *MYCN*-amplified NB cells;[9] thus targeting MYCN with BET inhibitors (BETis) may be efficient for the treatment of *MYCN*-amplified NB tumors.[9,10] In addition, *MYC* overexpression via enhancer activation drives a subset of high-risk NB.[11] These reports suggested BRD4 to be a therapeutic target in high-risk NB harboring *MYCN* amplification or *MYC* overexpression. On the other hand, clinical trials of BETis suggested that early acquired resistance to BETis limits their therapeutic benefit in solid tumors.[12,13]

MicroRNAs (miRNAs) are endogenous small non-coding RNAs of 20–25 nucleotides that repress the expression of their target genes post-transcriptionally by binding to complementary mRNA sequences. Nucleic acid therapeutics, including tumor-suppressive miRNA formulations, are now being developing as a next-generation treatment for cancer.[14,15] We previously identified *miR-3140-3p* as a potent candidate for nucleic acid therapeutics for cancer by function-based screening.[16,17] Administration of *miR-3140-3p* suppressed *in vivo* tumor growth in pancreatic cancer by concurrently targeting *BRD4, EGFR,* and *CDK2*.[16] In *MYCN*-amplified NB cells, the inhibition of CDK2 was reported to induce synthetic lethality.[18] EGFR inhibitors suppress tumor growth in a subset of NB tumors.[19,20] As *miR-3140-3p* concurrently targets *BRD4, EGFR,* and *CDK2*, we hypothesized that *miR-3140-3p* can inhibit tumor cell growth efficiently and overcome the resistance to BETi in NB cells. In the present study,
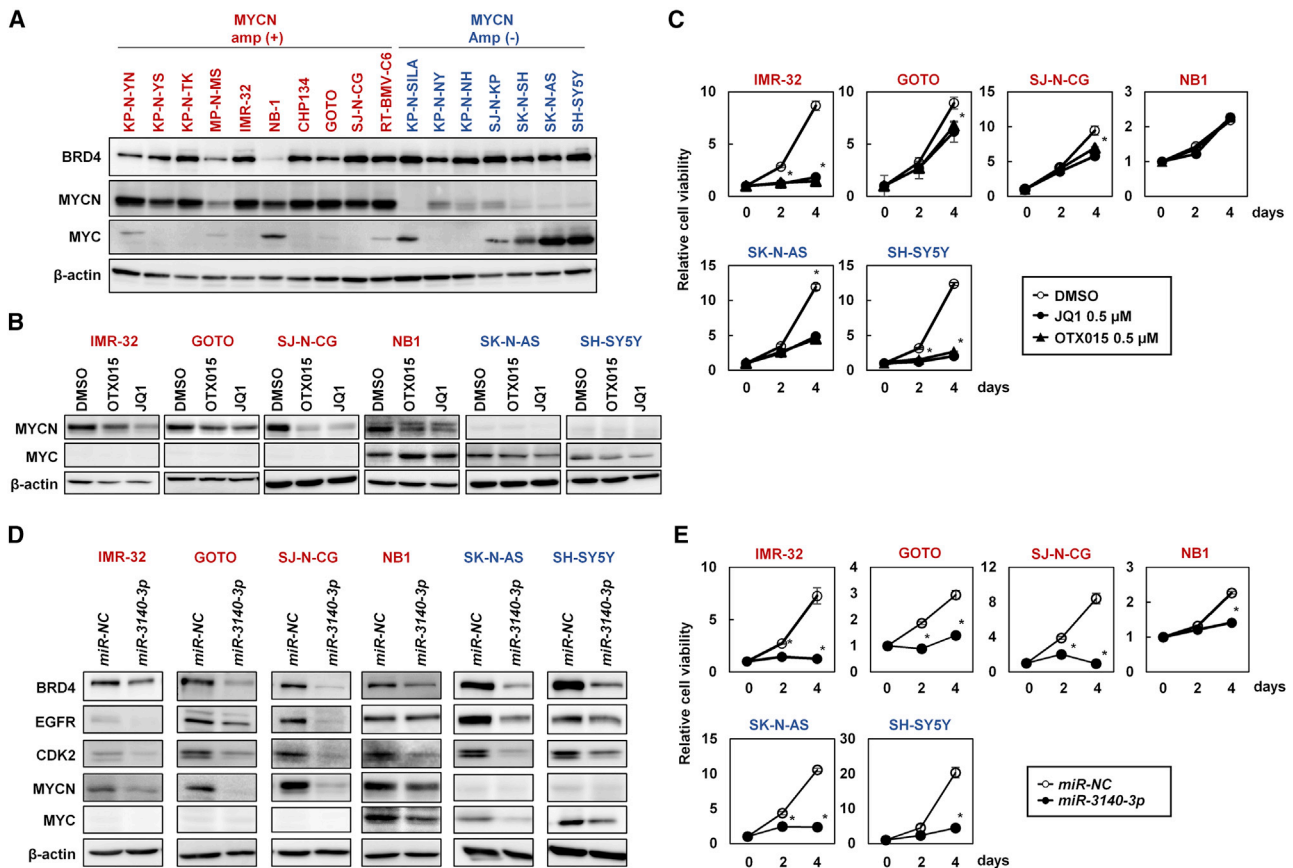
Figure 1. Comparison of the tumor-suppressive effects between the BETi and *miR-3140-3p* in neuroblastoma cells

(A) western blot analysis of BRD4, MYCN, and MYC with β-actin as a loading control in a panel of neuroblastoma (NB) cells. Red, *MYCN* amplified cell lines. Blue, *MYCN* non-amplified cell lines. Green, *MYC* amplified cell line. (B and C) Western blotting (B) and cell growth assay (C) of indicated cell lines after treatment with DMSO or 0.5 μmol/L OTX015 or JQ1. The cell growth rate was assessed by WST-8 assay using a relative ratio compared with day 0. Bar, SD for triplicate experiments. *p < 0.05. (D and E) Western blotting (D) and cell growth assay (E) of indicated cell lines after transfection with 10 nmol/L *miR-NC* or *miR-3140-3p*. The cell growth rate was assessed by WST-8 assay using a relative ratio compared with day 0. Bar, SD for triplicate experiments. *p < 0.05.

we compared the effects of *miR-3140-3p* with BETi on growth suppression in high-risk NB cells. We revealed the mechanisms of acquired resistance to BETi in NB cells by establishing BETi-acquired resistant NB cells. Finally, we demonstrated that *miR-3140-3p* has the potential to overcome BETi-acquired resistance by suppressing the newly identified target *MAP3K3* in NB cells.

RESULTS

BETi inhibited *in vitro* cell growth by suppressing MYCN or MYC through BRD4 inhibition in *MYCN*-amplified or MYC-elevated NB cells

We first determined the protein expression levels of BRD4, MYCN, and MYC in a panel of 17 NB cell lines by western blotting. As shown in Figure 1A, the expression of MYCN was upregulated in *MYCN*-amplified NB cells, although that of MYCN was slightly detected in MP-N-MS. MYCN was also detected in 3 MYCN-non-amplified NB cell lines (KP-N-NY, KP-N-NH, and SJ-N-KP). On the other hand, MYC expression increased in 1 *MYCN*-amplified NB cell line

(NB-1) and 5 MYCN-non-amplified NB cell lines (KP-N-SILA, SJ-N-KP, SK-N-SH, SK-N-AS, and SH-SY5Y) (Figure 1A).

Next, the effects of BETi on the expression of MYCN and MYC were examined in NB cells as follows: four *MYCN*-amplified NB (IMR-32, GOTO, SJ-N-CG, MP-N-MS), one *MYCN*-amplified and MYC-elevated NB (NB-1), and two MYC-elevated NB (SK-N-AS and SH-SY5Y) cell lines. Treatment with 0.5 μmol/L of BETi (JQ1 and OTX015) reduced the expression of MYCN and MYC in *MYCN*-amplified NB cells (IMR32, GOTO, SJ-N-CG, MP-N-MS, and NB-1) and MYC-elevated NB cells (SK-N-AS and SH-SY5Y), respectively (Figures 1B and S1A). Of note, the expression of MYC paradoxically increased after treatment with BETi in NB-1 cells (Figure 1B). This paradoxical increase in MYC was also observed after knocking down *BRD4* or *MYCN* with small interfering RNA (siRNA) in NB-1 cells (Figures S1B and S1C). Consequently, 0.5 μmol/L of JQ1 and OTX015 suppressed *in vitro* cell growth of all NB cell lines tested except for NB-1 cells, which were intrinsically resistant to BETi (Figure 1C).

These effects of BETi were similar to those of siRNA targeting *BRD4* (Figures S1B and S1D), suggesting that the effects of BETi are mainly due to the inhibition of BRD4, as previously reported.[21]

miR-3140-3p suppressed *in vitro* cell growth in *MYCN*-amplified or MYC-elevated NB cells

To compare the effects of *miR-3140-3p* with BETi, we transfected the same NB cell lines used for BETi treatment with 10 μM *miR-3140-3p*. The expression of BRD4, EGFR, and CDK2, which are known direct targets of *miR-3140-3p*,[19] was reduced in *miR-3140-3p*-transfected NB cells (Figures 1D and S2). *miR-3140-3p* downregulated the expression of MYCN and MYC in *MYCN*-amplified NB cells and MYC-elevated NB cells, respectively (Figure 1D). Of note, *miR-3140-3p* suppressed both MYCN and MYC expression in intrinsically BETi-resistant NB-1 cells (Figures 1B and 1C). Accordingly, *miR-3140-3p* suppressed the *in vitro* cell viability of all NB cell lines tested (Figures 1E and S2).

Establishment of BETi-acquired resistant NB cells

To examine the mechanism of acquired resistance to BETi in NB cells, JQ1-resistant-IMR-32 (IMR-32-JQ1R) and OTX015-resistant-GOTO (GOTO-OTXR) cells were generated from IMR-32 and GOTO cells, respectively. We selected IMR-32 and GOTO cells to generate BETi-resistant NB cells since these cells were easy to culture for long periods. As shown in Figures 2A and 2B and Figure S3A, IMR-32-JQ1R and GOTO-OTXR cells were tolerant to JQ1 and OTX015, respectively. Moreover, IMR32-JQ1R cells were resistant to OTX015, indicating that IMR32-JQ1R cells acquired cross-resistance to OTX015 (Figures 2A and 2B). Similarly, cross-resistance to JQ1 was observed in GOTO-OTXR cells (Figure S3A). This suggested that IMR32-JQ1R and GOTO-OTXR cells acquired resistance to BETi.

The expression of MYCN protein, but not MYCN mRNA, was only slightly reduced by JQ1 or OTX015 in IMR-32-JQ1R and GOTO-OTXR cells, whereas that of MYCN protein was reduced by JQ1 and OTX015 in a dose-dependent manner in IMR-32 and GOTO cells (Figures 2C and 2D; Figure S3B). Knockdown of MYCN by siRNA suppressed cell viability of IMR32-JQ1R and GOTO-OTXR cells and their parental cells (Figures 2E and S3C), suggesting that insufficient reduction of MYCN protein after BETi treatment played a role in the acquired resistance to BETi.

MYCN protein was stabilized because of reduced ubiquitin-mediated proteolysis in BETi-acquired resistant NB cells

We found that IMR-32-JQ1R cells proliferated faster than IMR-32 cells (Figure 2F). As mitogen-activated protein kinase (MAPK)/ERK1/2 signaling and phosphatidylinositol 3-kinase (PI3K)/AKT signaling are key proliferative pathways, we examined the levels of activated ERK1/2 (phosphorylated ERK1/2 [p-ERK1/2] [Thr202/Tyr204]) and activated AKT (phosphorylated AKT [p-AKT] [Ser473]) in these cells. As a result, the expression of p-ERK1/2, but not p-AKT, was markedly higher in IMR-32-JQ1R cells than in IMR-32 cells (Figure 2G). A similar increase in p-ERK1/2 was observed in GOTO-OTXR cells (Figure S3D).

Based on previous reports that activated ERK1/2 stabilizes MYCN protein by preventing ubiquitin-mediated proteolysis via phosphorylation of MYCN at Ser62,[22,23] we hypothesized that the stability of MYCN protein increased in IMR-32-JQ1R cells. The expression of phosphorylated MYCN (p-MYCN) (Ser62) increased in IMR-32-JQ1R cells (Figure 2G). Cycloheximide chase assay demonstrated that the half-life of MYCN protein was significantly longer in IMR-32-JQ1R cells than in IMR-32 cells (IMR-32: 34.8 ± 9.6 min, IMR-32-JQ1R: 57.1 ± 7.4 min, p = 0.03) (Figure 3A). In addition, ubiquitinated MYCN was reduced in IMR-32-JQ1R cells compared with IMR-32 cells (Figure 3B). Collectively, the stability of MYCN was higher because of reduced ubiquitin-mediated proteolysis in IMR-32-JQ1R cells. Similar results were obtained in GOTO-OTXR cells (Figures S3D, S4A, and S4B).

Activated ERK1/2 conferred resistance to BETi by stabilizing MYCN in BETi-acquired resistant NB cells

We next examined whether activated ERK1/2 stabilized MYCN protein in IMR-32-JQ1R cells. As shown in Figures 3C and 3D, the MEK inhibitor trametinib or transfection of siRNA targeting *ERK1* and *ERK2* reduced p-ERK1/2 in IMR-32 and IMR-32-JQ1R cells. As a result, p-MYCN (Ser62) and MYCN decreased through the downregulation of p-ERK1/2 in IMR-32-JQ1R cells but not in IMR-32 cells (Figures 3C–3E). Concordantly, trametinib increased ubiquitinated MYCN in IMR-32-JQ1R cells (Figure 3F). Proteasome blockade with MG132 rescued the expression of MYCN protein, but not MYCN mRNA, in the presence of trametinib in IMR-32-JQ1R cells, supporting the promotion of ubiquitin-mediated proteolysis by trametinib (Figures S5A and S5B). Similarly, ubiquitination of MYCN increased with the decrease in p-MYCN (Ser62) after trametinib treatment in GOTO-OTXR cells (Figures S6A and S6B). This suggested that activated ERK1/2 stabilizes MYCN protein by preventing ubiquitin-mediated proteolysis via phosphorylation of MYCN at Ser62 in BETi-acquired resistant NB cells.

Moreover, the combination of trametinib with JQ1 or OTX015 cooperatively suppressed cell viability with the downregulation of MYCN in IMR-32-JQ1R and GOTO-OTXR cells (Figures 3G and S6C), suggesting that the addition of trametinib restored sensitivity to BETi in these cells. Taken together, activation of ERK1/2 conferred BETi-acquired resistance by stabilizing MYCN in NB cells.

miR-3140-3p suppressed tumor cell growth in BETi-acquired resistant NB cells

To assess whether *miR-3140-3p* can overcome the acquired resistance to BETi in NB cells, we examined the effects of *miR-3140-3p* on the expression of MYCN, p-MYCN (Ser62), and p-ERK1/2 in IMR-32-JQ1R and GOTO-OTXR cells. As shown in Figures 4A, S7, and S8A, the expression of MYCN, p-MYCN (S62), p-ERK1/2, BRD4, EGFR, and CDK2 was downregulated by *miR-3140-3p* in IMR-32-JQ1R and GOTO-OTXR cells. *miR-3140-3p* increased ubiquitinated MYCN, and this increase was cancelled by *miR-3140-3p inhibitor* in IMR-32-JQ1R cells (Figure S8B). Consequently, *miR-3140-3p* suppressed tumor cell growth in both IMR-32-JQ1R and
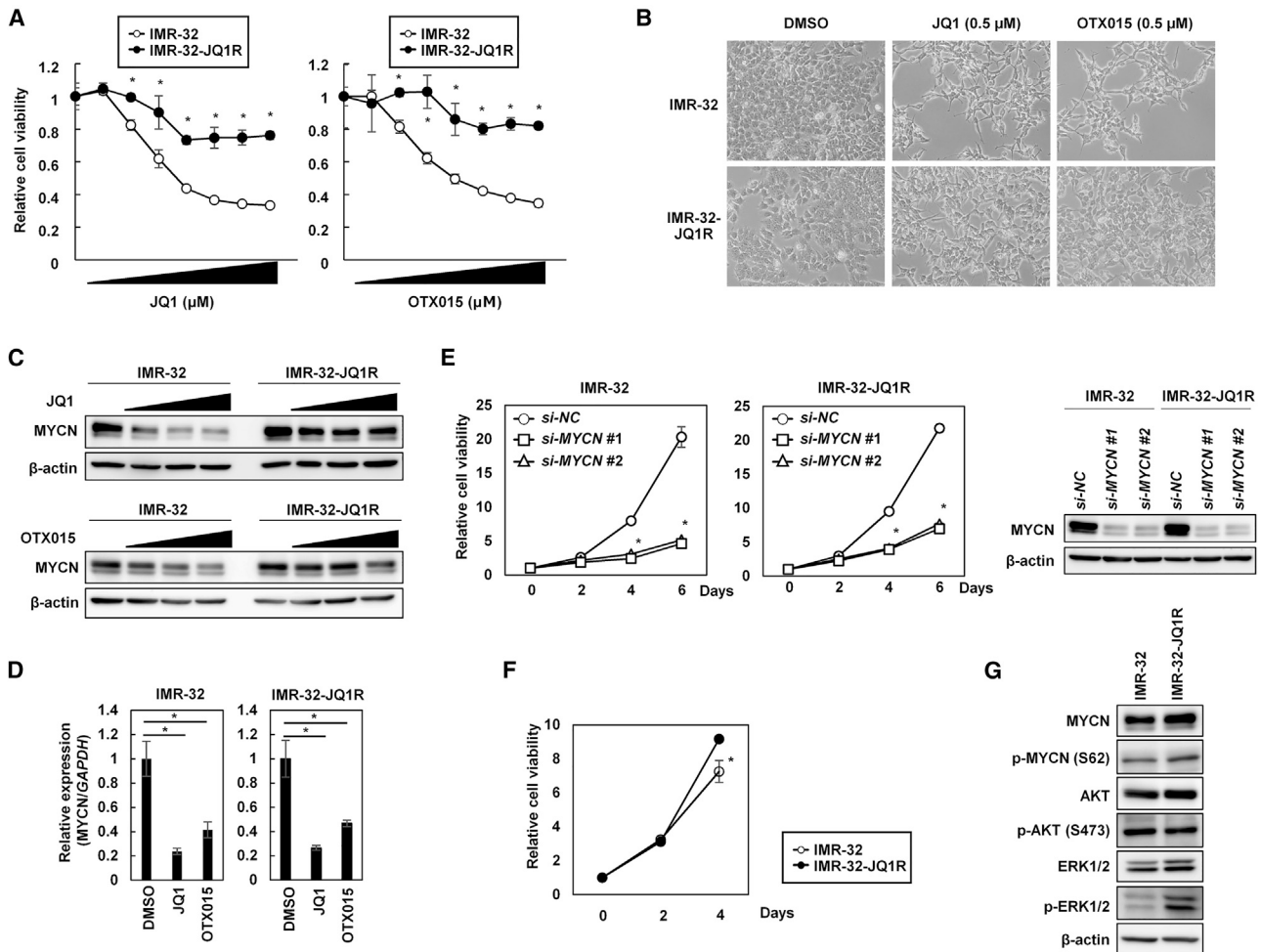
Figure 2. Establishment of BETi-resistant IMR-32 (IMR-32-JQ1R) cells

(A) Dose-response curve for cell viability using WST-8 assay of IMR-32 and IMR-32-JQ1R cells treated with different concentrations (0, 0.031, 0.063, 0.13, 0.25, 0.50, 1.0, and 2.0 μmol/L) of JQ1 or OTX015 for 48 h. Data represent means and SD of two independent experiments performed in triplicate. (B) Phase-contrast images of IMR-32 and IMR-32-JQ1R cells after treatment with DMSO or JQ1 or OTX015 at 0.5 μmol/L for 48 h. (C) Western blot analysis of MYCN expression in IMR-32 and IMR-32-JQ1R cells 48 h after treatment with JQ1 (upper) or OTX015 (lower) at 0, 0.25, 0.50, or 1.0 μmol/L. (D) Relative expression of MYCN mRNA assessed by qRT-PCR in IMR-32 and IMR-32-JQ1R after treatment with DMSO or JQ1 or OTX015 at 0.50 μmol/L for 48 h. Bar, SD for triplicate experiments. *p < 0.05. (E) Western blot analysis (right) and cell growth assay (left) of IMR32 and IMR32-JQ1R cells after transfection with si-NC, si-MYCN #1, or si-MYCN #2 (each 20 nmol/L). The cell growth rate was assessed by WST-8 assay using a relative ratio compared with day 0. Bar, SD for triplicate experiments. *p < 0.05. (F) In vitro cell growth of IMR-32 and IMR-32-JQ1R cells. The cell growth rate was assessed by WST-8 assay using a relative ratio compared with day 0. Bar, SD for triplicate experiments. *p < 0.05. (G) Western blot analysis of the indicated proteins in IMR-32 and IMR-32-JQ1R cells.

GOTO-OTXR cells, as well as in their parental cells (Figures 4B, 4C, and S8C). Cell cycle analysis suggested that *miR-3140-3p* might induce G1 arrest in these cells (Figures S9A and S9B).

miR-3140-3p directly targeted the MAP3K3-ERK1/2 pathway in NB cells

We next examined the mechanism by which *miR-3140-3p* suppressed p-ERK1/2 in BETi-acquired resistant NB cells. As knockdown of EGFR did not affect the level of p-ERK1/2 in IMR-32-JQ1R cells (Figure S10A), novel targets of *miR-3140-3p* were explored. According to our previous screening on targets of *miR-3140-3p* using gene expres-

sion array analysis combined with TargetScan database research,[19] several genes of the MAPK/ERK1/2 pathway, including *MAP2K1*, *MAP3K2*, and *MAP3K3*, were potentially targeted by *miR-3140-3p*. Among these 3 genes, MAP3K3 expression, which increased in BETi-acquired resistant cells (Figure S10B), was markedly downregulated by *miR-3140-3p* in IMR-32-JQ1R and GOTO-OTXR cells (Figures 4A and S8A). Knockdown of MAP3K3 using siRNA partially restored the sensitivity to BETi with decreased expression of p-ERK1/2 in both BETi-acquired resistant NB cell lines (Figures 4D, S10C, and S10D). Conversely, overexpression of MAP3K3 in IMR-32 cells conferred resistance to BETi with increased levels of
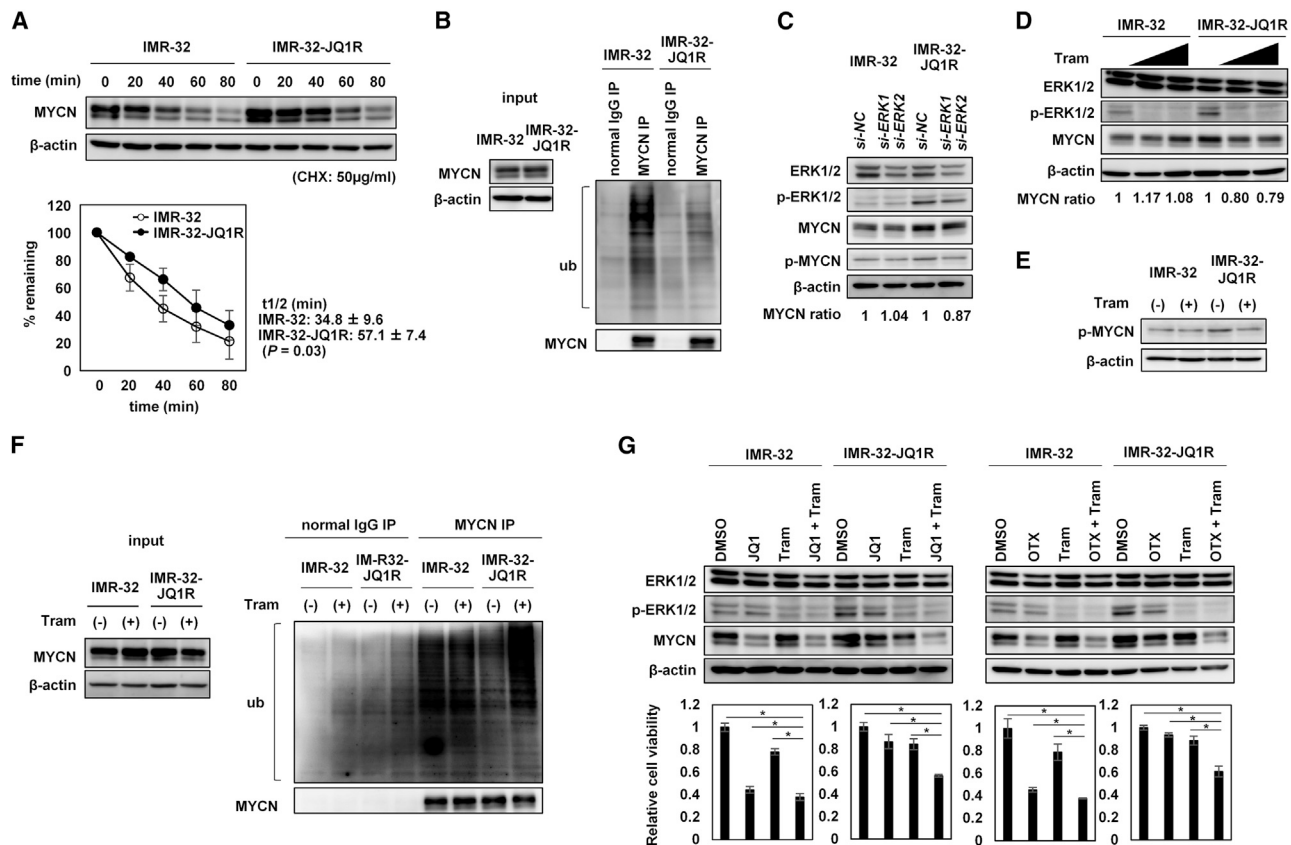
Figure 3. Activated ERK1/2 conferred resistance to BETi by stabilizing MYCN in BETi-acquired resistant NB cells

(A) Cycloheximide (CHX) chase assay showing the half-life of MYCN in IMR-32 and IMR-32-JQ1R cells. Cells were harvested at the indicated time points after CHX addition and subjected to western blotting with antibodies against MYC and β-actin (upper). The percentage of MYCN remaining at each time point was quantitated by ImageJ software (lower). The values were normalized against β-actin for each sample. Bar, SD for 3 independent experiments. (B) Ubiquitinated MYCN in IMR-32 and IMR-32-JQ1R cells. Protein lysates were immunoprecipitated with the anti-MYCN antibody. Amounts of polyubiquitin were measured by immunoblotting with an anti-ubiquitin antibody. (C–E) Western blotting of indicated protein in IMR-32 and IMR-32-JQ1R cells. Cells were treated with trametinib at indicated concentrations (C and D) or transfected with *si-NC* or *si-ERK1/si-ERK2* (E). The intensity of MYCN bands was quantified by densitometry and shown as the fold change after normalization (C and E). These experiments were repeated three times. (F) Ubiquitinated MYCN in IMR-32 and IMR-32-JQ1R cells treated with DMSO or trametinib (Tram, 1.0 μmol/L). Amounts of polyubiquitin were measured as described in (B). (G) Western blot analysis (upper) and cell growth assay (lower) of IMR-32 and IMR-32-JQ1R cells after treatment with DMSO, BETi (JQ1 or OTX015), trametinib, or the combination of BETi and trametinib (BETi: 0.50 μmol/L, trametinib: 1.0 μmol/L). The cell growth rate was assessed by WST-8 assay using a relative ratio compared with that of DMSO-treated cells. Bar, SD for triplicate experiments. *p < 0.05.

p-ERK1/2 and p-MYCN (S62) (Figure 4E). Accordingly, the stability of MYCN increased with decreased levels of ubiquitinated MYCN in MAP3K3-overexpressed IMR-32 cells (Figures 4F and 4G). This suggested that overexpression of MAP3K3, at least in part, played a role in the acquired resistance to BETi in NB cells.

In luciferase assays using reporter plasmid vectors with wild-type (WT) or mutant (Mt) sequences of the 3¿ UTRs of *MAP3K3*, the luciferase activity was significantly reduced by *miR-3140-3p* with the WT vector compared with the empty vector (EV), whereas it was restored with the Mt vector (Figure 4H). This suggested that *miR-3140-3p* directly targets *MAP3K3* by binding to its 3¿ UTR. Thus, *miR-3140-3p* overcame the acquired resistance to BETi by concurrently targeting BRD4 and the MAP3K3-ERK1/2 pathway in NB cells.

DISCUSSION

We demonstrated that *miR-3140-3p* suppresses tumor cell growth in *MYCN*-amplified NB cells, including NB1 cells that have intrinsic resistance to BETi. We further revealed that the acquired resistance to BETi was through the stabilization of MYCN protein due to activated ERK1/2 in NB cells. Finally, *miR-3140-3p* downregulated MYCN expression transcriptionally by suppressing BRD4 and post-transcriptionally through the MAP3K3-ERK1/2 pathway, thereby overcoming the acquired resistance to BETi in NB cells (Figure 5).

According to the TARGET (Therapeutically Applicable Research To Generate Effective Treatments) database, in high-risk NB, high-level amplification of *MYCN* or *MYC* was observed in 35.5% or 0.4%, respectively (https://ocg.cancer.gov/programs/target; Tables S1 and
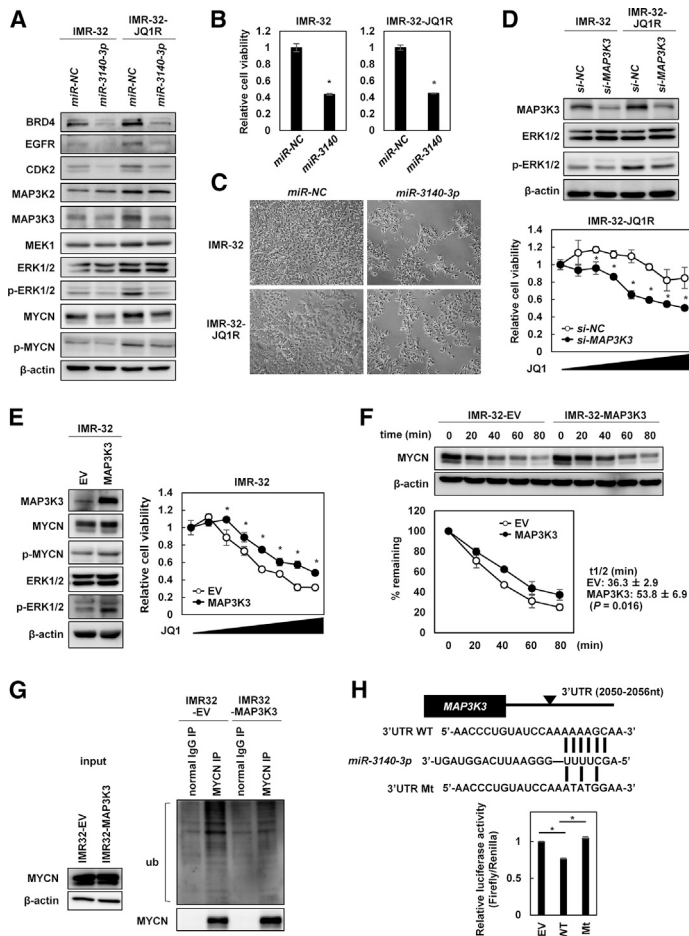
Figure 4. *miR-3140-3p* suppressed the growth of BETi-acquired resistant NB cells by concurrently targeting BRD4 and the MAP3K3-ERK1/2 pathway
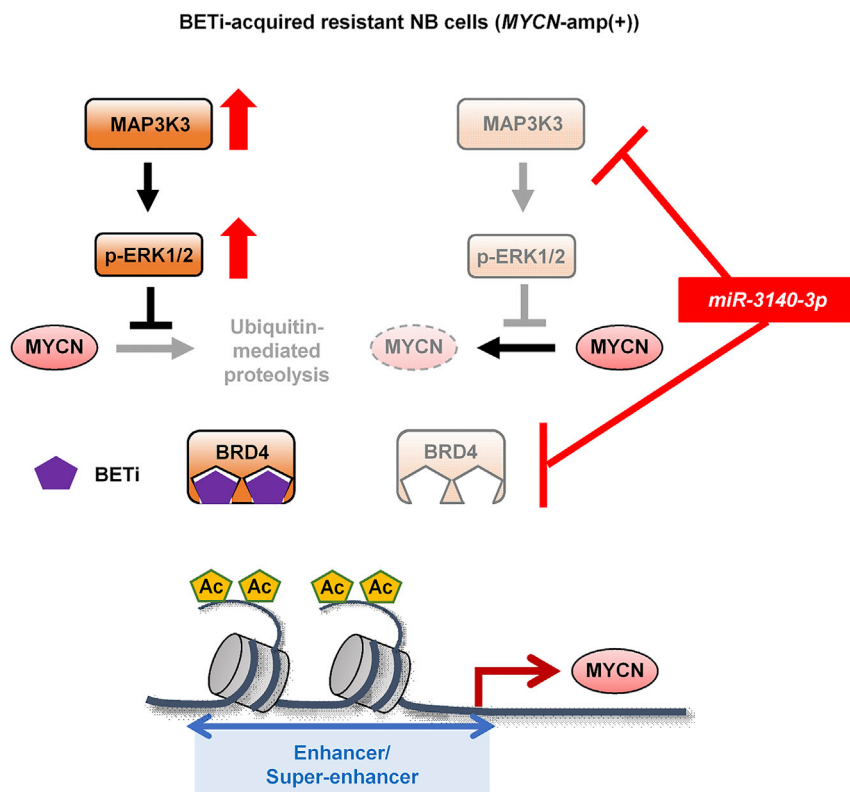
(A) Western blotting of the indicated proteins in IMR-32 and IMR-32-JQ1R cells transfected with 10 nmol/L *miR-NC* or *miR-3140-3p*. (B) Cell growth assay (upper) and phase-contrast images (lower) of IMR-32 and IMR-32-JQ1R cells 72 h after transfection with 10 nmol/L *miR-NC* or *miR-3140-3p*. The cell growth rate was assessed by WST-8 assay using a relative ratio compared with *miR-NC*-transfected cells. Bar, SD for triplicate experiments. * *P* < 0.05. (C) Western blotting for MAP3K3, ERK1/2, and p-ERK1/2 in IMR-32 and IMR-32-JQ1R cells transfected with 20 nmol/L *si-NC* or *si-MAP3K3*. (D) Dose-response curve for cell viability using the WST-8 assay in IMR-32-JQ1R cells after treatment with different concentrations (0, 0.031, 0.063, 0.13, 0.25, 0.50, 1.0, or 2.0 μmol/L) of JQ1 for 48 h combined with transfection with *si-NC* or *si-MAP3K3*. The cell growth rate was assessed using a relative ratio compared with that of DMSO-treated cells. Bar, SD for triplicate experiments. * *P* < 0.05. (E) Western blotting of the indicated proteins in control cells (IMR-32-EV) and MAP3K3-overexpressing stable clone (IMR-32-MAP3K3). Dose-response curve for cell viability using the WST-8 assay in IMR-32-EV and IMR-32-MAP3K3 cells after treatment with different concentrations (0, 0.031, 0.063, 0.13, 0.25, 0.50, 1.0, or 2.0 μmol/L) of JQ1 for 48 h. The cell growth rate was assessed using a relative ratio compared with that of DMSO-treated cells. Bar, SD for triplicate experiments. * *P* < 0.05. (F) Cycloheximide (CHX) chase assay of IMR-32-EV and IMR-32-MAP3K3 cells, as described in Figure 3A. Western blotting (upper) and the quantification of MYCN at each time point (lower). The values were normalized against β-actin for each sample. Bar, SD for 3 independent experiments. (G) Ubiquitinated MYCN in IMR-32-EV and IMR-32-MAP3K3 cells. Amounts of poly-ubiquitin were measured as described in Figure 3B. (H) Luciferase reporter assays. IMR-32 cells were cotransfected with pmirGLO dual-luciferase vectors containing the wild-type (WT) 3′UTRs of *MAP3K3* or mutant variants (Mt) of *MAP3K3* and *miR-NC* or *miR-3140*. Upper, a putative binding site of *miR-3140* within the 3′UTR of *MAP3K3* and mutant sequences. Lower, the results of the luciferase assay; **P* < 0.05.

S2). We first revealed that *miR-3140-3p* suppresses *in vitro* tumor cell growth in *MYCN*-amplified and MYC-elevated NB cells. In contrast to BETi, *miR-3140-3p* suppressed tumor cell growth in NB-1 cells that exhibited intrinsic resistance to BETi due to the paradoxical increase in MYC expression after BETi treatment. A similar paradoxical increase in MYC by BETi treatment was reported to be associated with ERK1/2 activation in MYCN-overexpressed triple-negative breast cancer cells.[24] Consistent with this report, concurrent suppression of p-ERK1/2 and BRD4 by *miR-3140-3p*, as well as the combined treatment of trametinib with BETi, downregulated both MYCN and MYC expression, thereby suppressing tumor cell growth of NB-1 cells (Figures S11A and S11B). Although further examination is needed to reveal the mechanism by which activated ERK1/2 instead of BRD4 upregulated MYC in NB-1 cells, ERK1/2 activation may be associated with less intrinsic sensitivity to BETi. As RAS-MAPK activation is frequently induced by genomic alteration, such as *ALK*, *NF1*, and *PTPN11*, in high-risk NB,[25] a strategy of simultaneously targeting the ERK1/2 pathway and BRD4 may be rational for the treatment of high-risk NB.

We revealed that the stabilization of MYCN protein due to activation of ERK1/2 conferred acquired resistance to BETi in NB cells.

The stability of MYCN and MYC was reported to be regulated by p-ERK1/2-mediated phosphorylation of MYCN at Ser62.[22,23] Our study results are consistent with these reports. We further revealed that activated ERK1/2 attenuates the effects of BETi via MYCN stabilization in BETi-acquired resistant NB cells. In contrast to our results, receptor tyrosine kinase/PI3K activation was reported to be associated with BETi resistance in genome-scale, pooled lentiviral open reading frame and CRISPR knockout rescue experiments in NB cells.[26] These differences may be due to differences in the experimental model. Several mechanisms of acquired resistance to BETi were reported in different types of cancer: WNT/β-catenin activation promotes MYC transcription instead of BRD4 in acute leukemia cells;[27] activation of receptor tyrosine kinases stabilizes MYC and FOSL1 in ovarian cancer cells;[28] and loss of PP2A-induced hyperphosphorylation of BRD4 strengthens the transcription of MYC in triple-negative breast cancer cells.[29] Stabilization of MYCN induced by p-ERK1/2 may be one of the novel mechanisms of acquired resistance to BETi in NB.

Finally, we demonstrated that *miR-3140-3p* suppresses p-ERK1/2, at least in part, by directly targeting MAP3K3. A previous study

BETi-acquired resistant NB cells (*MYCN*-amp(+))

Figure 5. Diagram summarizing the mechanism by which *miR-3140-3p* overcomes the acquired resistance to BETi in NB cells

Activation of the MAP3K3-ERK1/2 pathway conferred BETi-acquired resistance by stabilizing MYCN in NB cells. *miR-3140-3p* downregulated MYCN expression transcriptionally by suppressing BRD4 and post-transcriptionally through the MAP3K3-ERK1/2 pathway, thereby overcoming the acquired resistance to BETi in NB cells.

revealed that MAP3K3 directly activates the ERK1/2 pathway.[30] MAP3K3 regulates p-ERK1/2 in several cellular contexts, including osteogenesis,[31] immflamation,[32] proliferation,[33] and differentiation.[34] In breast cancer, amplification and overexpression of *MAP3K3* have been reported to lead to carcinogenesis.[35] Moreover, activated ALK promotes MYC transcription through the MAP3K3-ERK5 pathway in ALK-positive NB cells.[36] These reports support MAP3K3 as a potential therapeutic target for NB, although further assessment of the clinical relevance of MAP3K3 is required in NB. Interestingly, we found that knockdown of MYCN increased the expression of MAP3K3 and p-ERK1/2 in IMR-32, GOTO, and their BETi-resistant cells (Figure S12). Although the mechanism by which silencing MYCN upregulated MAP3K3 and p-ERK1/2 was unknown, these results suggested that concurrent suppression of BRD4-MYCN and MAP3K3-p-ERK1/2 pathway by *miR-3140-3p* might be rational for the treatment of NB.

The expression of *miR-3140-3p* was barely detectable in normal adrenal tissue and panels of NB cells and BETi-acquired resistance NB cells, whereas that of *miR-3140-3p* increased thousands of times to exert its function in *miR-3140-3p*-transfected cells (Figure S13). The expression of endogenous *miR-3140-3p* might be too low to function in these NB cells. In addition, although the data of *miR-3140-3p* does not exist in primary NB tumors in a TARGET study or TCGA study, the expression of *miR-3140-3p* was extremely low both in other types of cancers and normal tissues compared with

that of the representative miRNA *miR-34a-5p* or *let-7a-5p* (Table S3). The expression of endogenous *miR-3140-3p* would be expected to be low also in NB tumors. Further analysis is needed to reveal the expression and biological function of endogenous *miR-3140-3p*.

In conclusion, our study demonstrated that *miR-3140-3p* efficiently downregulates the expression of both MYCN and MYC by concurrently targeting BRD4 and the MAP3K3-ERK1/2 pathway in NB cells. Unfortunately, BETi-resistant NB cells and their parental cells used in this study could not form subcutaneous tumors in our xenograft model. Although further studies, including *in vivo* experiments, are required to evaluate the therapeutic potential of *miR-3140-3p* for NB tumors, *miR-3140-3p* has the potential to overcome the intrinsic or acquired resistance to BETi in NB cells.

MATERIALS AND METHODS

Cell culture

KP-N-YN, KP-N-YS, KP-N-TK, MP-N-MS, KP-N-RT-BMV6, KP-N-SILA, KP-N-NY, KP-N-NH, SJ-N-CG, SJ-N-KP, and SK-N-AS cells, which were established as described previously,[37–39] were gifts from Dr. Tohru Sugimoto (Kyoto Prefectural University of Medicine). These cell lines were authenticated by monitoring cell morphology. NB-1, GOTO, and IMR-32 were obtained from the JCRB Cell Bank (Tokyo, Japan). CHP134 was purchased from the RIKEN Cell Bank (Osaka, Japan). SH-SY5Y was from ATCC (Manassas, VA, USA). The identities of IMR-32, GOTO, NB-1, SH-SY5Y, and CHP-134 cell lines were authenticated by short tandem repeat profiling by BEX CO., Ltd. All cell lines used in this study were cultured in RPMI1640 medium containing 10% fetal bovine serum (FBS) at 37°C in 5% CO_2 for no more than 20 passages from the validated stocks. The status of *MYCN* amplification in NB cell lines used in this study was determined previously.[40] All experiments were carried out in accordance with the approved guidelines and regulations (G2019-013A).

Reagents

JQ1, OTX015, trametinib, and MG132 were purchased from Selleck Chemicals (Houston, TX, USA), and cycloheximide was obtained from WAKO Pure Chemical Industries (Tokyo, Japan). These

reagents were used for the treatment of cultured cells *in vitro* at the indicated concentrations.

Transfection of miRNAs and siRNAs

The double-stranded RNAs (dsRNAs) mimicking mature human *miR-3140-3p* (MC17496), a non-specific control miRNA (negative control #1), and *miR-3140-3p inhibitor* (MH17496) were purchased from Thermo Fisher Scientific (Waltham, MA, USA). The SMART-pool siRNAs for *BRD4* (M-004937-02), ERK1 (*MAPK3*) (M-003592-03), ERK2 (*MAPK1*) (M-003555-04), *EGFR* (M-003114-03), and *MAP3K3* (M-003301-02) and nonspecific control siRNAs were obtained from GE Healthcare (Little Chalfont, Buckinghamshire, UK). Each SMARTpool siRNA contains 4 siRNA duplexes designed to target different mRNA sequences of the same gene. siRNAs targeting *MYCN* (#1, s9133; #2, s526555) were from Thermo Scientific. miRNAs and siRNAs were transfected individually into cells at the indicated concentrations with Lipofectamine RNAiMAX (Thermo Fisher Scientific) according to the manufacturer's instructions.

In vitro cell growth assay

Cell viability was evaluated by the WST-8 assay (Cell Counting Kit-8; Dojindo, Kumamoto, Japan) as described previously.[19] Each assay was carried out in triplicate.

Cell cycle analysis

The cell cycle was evaluated 48 h after transfection of *miR-NC* or *miR-3140-3p* (each 10 nmol/L) in IMR-32, IMR-32-JQ1R, GOTO, and GOTO-OTXR cells by flow cytometry as previously described.[41]

Western blotting

Western blotting was performed as previously described.[42] The following primary antibodies were used for western blotting: antibodies against BRD4 (#13440), MYC (#9402), MYCN (#51705), p-ERK1/2 (Thr202/Tyr204) (#4370), ERK1/2 (#4695), AKT (#9272), p-AKT (Ser473) (#4060), and MAP3K3 (#5727) were purchased from Cell Signaling Technology (Danvers, MA, USA); anti-MAP3K2 was from Proteintech (Chicago, IL, USA); the antibody against phosphorylated MYC (Ser62) (ab51156), which was used to detect p-MYCN (Ser62) in NB cells as previously reported,[22] was obtained from Abcam (Cambridge, UK); antibodies against CDK2 (sc-163) and EGFR (sc-03-G) were from Santa Cruz Biotechnology (Dallas, TX, USA); anti-β-actin (A5441) was obtained from Sigma-Aldrich (Tokyo, Japan).

Establishment of BETi-acquired resistant NB cells

BETi-acquired resistant cells derived from IMR-32 and GOTO cells were established by long-term incubation with gradually increasing JQ1 or OTX015 (i.e., BETi) concentrations, respectively. The cells were initially exposed to BETi at 0.1 μmol/L in RPMI medium, cultured in BETi-free medium to confluence, and then exposed to BETi at a higher concentration. This cycle was repeated for several months. IMR-32 or GOTO cells that were able to survive in RPMI medium containing 2.0 μmol/L JQ1 or OTX015 were defined as IMR-32-JQ1R or GOTO-OTXR cells, respectively.

Luciferase activity assay

The luciferase activity assay was carried out as previously described.[19] In brief, luciferase reporter plasmids were constructed by inserting the 3′ UTRs of *MAP3K3* downstream of the luciferase gene in the pmir-GLO Dual-Luciferase miRNA Target Expression Vector (Promega, Madison, WI, USA). All site-specific mutations were generated by the KOD-Plus-Mutagenesis Kit (TOYOBO, Osaka, Japan). Firefly and *Renilla* luciferase activities were measured with the Dual-Luciferase Reporter Assay System (Promega), and relative luciferase activity was calculated by normalizing the firefly luciferase reading to its corresponding internal *Renilla* luciferase control.

Cycloheximide chase assay

To assess MYCN protein stability, a cycloheximide chase assay was performed. Cells were treated with cycloheximide (50 μg/mL) (Sigma-Aldrich) for the indicated time periods prior to cell harvesting. The amount of MYCN at each time point was analyzed by western blotting. Band intensities of MYCN were calculated by ImageJ software (National Institutes of Health, Bethesda, MA, USA), and the values were normalized against β-actin for each sample. Cycloheximide chase experiments were repeated for three independent biological replicates.

Detection of ubiquitinated MYCN

Ubiquitinated protein was detected as described previously.[43] Briefly, cells were lysed with cell lysis buffer (#9803, Cell Signaling Technology) with protease inhibitors, and the lysates were incubated with normal rabbit IgG and protein A magnetic beads (#73778, Cell Signaling Technology) for 30 min to reduce non-specific protein binding. After separation of the beads, the supernatant was incubated with anti-MYCN antibody or normal rabbit IgG (control) overnight on a rotator at 4°C. The lysate and antibody were then incubated with protein A magnetic beads. The immunoprecipitated protein complexes were analyzed by western blotting. Levels of ubiquitinated forms of MYCN were measured by immunoblotting with ubiquitin conjugates-specific HRP (Horseradish peroxidase)-linked antibody (Enzo Life Sciences, Tokyo, Japan).

Quantitative RT-PCR

Total RNA was extracted with TRIsure reagent (Bioline, London, UK) according to the manufacturer's instructions. Expression of mRNA was quantified by a real-time fluorescence detection method, as described previously.[44] The primers used were as follows: *MYCN* mRNA (forward, 5′-TCTACCCGGACGAAGATGAC-3′; reverse, 5′-CACAGCTCGTTCTCAAGCAG-3′). These primers were designed with Primer3 plus (https://primer3plus.com/) based on sequence data obtained from NCBI databases (https://www.ncbi.nlm.nih.gov/). The endogenous control for mRNA was *GAPDH*.

The expression of *miR-3140-3p* was examined as described previously.[16] The following primers were used for the TaqMan assay (Thermo Fisher Scientific): human *miR-3140-3p* (244524) and *RNU6B* (001093). Normal adrenal tissue RNA was purchased from BioChain Institute Inc. (Newark, CA, USA).

Establishment of MAP3K3-overexpressing cells

The complete coding sequence of *MAP3K3* was amplified from IMR-32 cells subcloned into the pCDH-CMV-MCS-EF1α-GreenPuro Cloning and Expression Lentivector (CD513B-1) (System Biosciences, Palo Alto, CA, USA) and verified by sequencing. Subsequently, lentiviral particles were produced with the pPACKH1 HIV Lentivector Packaging Kit (System Biosciences, LV500A-1) according to the manufacturer's instructions. IMR-32 cells were infected with the lentivirus and maintained in DMEM medium with puromycin (1 μg/mL) to select positive cells overexpressing MAP3K3 (IMR-32-MAP3K3 cells).

Public dataset analysis

To explore the copy number of MYCN and MYC, we examined the public datasets from TARGET (https://ocg.cancer.gov/programs/target) in 921 neuroblastoma primary samples. GISTIC analysis was performed with TARGET-30-combined_Illumina_915.seg file from the TARGET project under the following parameters; -refgene hg19.UCSC.add.miR.140312.refgene.mat -ta 0.1 -armpeel 1 -brlen 0.7 -cap 1.5 -conf 0.99 -td 0.1 -genegistic 1 -gcm extreme -js 4 -maxseg 2000 -qvt 0.25 -rx 0 -savegene 1. Summarized data of GISTIC are output as values of 0, 1, and 2. The values of 0, 1, and 2 indicate no amplification, low-level copy number amplification, and high-level copy number amplification, respectively.

To explore the expression of *miR-3140-3p*, *miR-34a-5p*, and *let-7a-5p* in various types of cancer, miRNA sequencing (miRNA-seq) data of the TCGA project were obtained from the ENCORI database (http://starbase.sysu.edu.cn/index.php).

Statistical analysis

Differences between groups were determined with the Student's t test and one-way ANOVA with Bonferroni adjustment, as appropriate. All statistical analyses were carried out with R software. p values of <0.05 were considered significant.

SUPPLEMENTAL INFORMATION

Supplemental information can be found online at https://doi.org/10.1016/j.omtn.2021.05.001.

AUTHOR CONTRIBUTIONS

C.L. and Y.G. were involved in the research design, performed the experiments, analyzed the data, and wrote the manuscript. K.T. contributed to public database analysis. T.M. and J. Inoue supervised the study. J. Inazawa was involved in the research design, wrote the manuscript, and supervised the study.

DECLARATION OF INTERESTS

The authors declare no competing interests.

REFERENCES

1. Matthay, K.K., Maris, J.M., Schleiermacher, G., Nakagawara, A., Mackall, C.L., Diller, L., and Weiss, W.A. (2016). Neuroblastoma. Nat. Rev. Dis. Primers 2, 16078.

2. Cohn, S.L., Pearson, A.D., London, W.B., Monclair, T., Ambros, P.F., Brodeur, G.M., Faldum, A., Hero, B., Iehara, T., Machin, D., et al.; INRG Task Force (2009). The International Neuroblastoma Risk Group (INRG) classification system: an INRG Task Force report. J. Clin. Oncol. 27, 289–297.

3. Maris, J.M. (2010). Recent advances in neuroblastoma. N. Engl. J. Med. 362, 2202–2211.

4. Whittle, S.B., Smith, V., Doherty, E., Zhao, S., McCarty, S., and Zage, P.E. (2017). Overview and recent advances in the treatment of neuroblastoma. Expert Rev. Anticancer Ther. 17, 369–386.

5. Kreissman, S.G., Seeger, R.C., Matthay, K.K., London, W.B., Sposto, R., Grupp, S.A., Haas-Kogan, D.A., Laquaglia, M.P., Yu, A.L., Diller, L., et al. (2013). Purged versus non-purged peripheral blood stem-cell transplantation for high-risk neuroblastoma (COG A3973): a randomised phase 3 trial. Lancet Oncol. 14, 999–1008.

6. Toyoshima, M., Howie, H.L., Imakura, M., Walsh, R.M., Annis, J.E., Chang, A.N., Frazier, J., Chau, B.N., Loboda, A., Linsley, P.S., et al. (2012). Functional genomics identifies therapeutic targets for MYC-driven cancer. Proc. Natl. Acad. Sci. USA 109, 9545–9550.

7. Chipumuro, E., Marco, E., Christensen, C.L., Kwiatkowski, N., Zhang, T., Hatheway, C.M., Abraham, B.J., Sharma, B., Yeung, C., Altabef, A., et al. (2014). CDK7 inhibition suppresses super-enhancer-linked oncogenic transcription in MYCN-driven cancer. Cell 159, 1126–1139.

8. Belkina, A.C., and Denis, G.V. (2012). BET domain co-regulators in obesity, inflammation and cancer. Nat. Rev. Cancer 12, 465–477.

9. Henssen, A., Althoff, K., Odersky, A., Beckers, A., Koche, R., Speleman, F., Schäfers, S., Bell, E., Nortmeyer, M., Westermann, F., et al. (2016). Targeting MYCN-Driven Transcription By BET-Bromodomain Inhibition. Clin. Cancer Res. 22, 2470–2481.

10. Puissant, A., Frumm, S.M., Alexe, G., Bassil, C.F., Qi, J., Chanthery, Y.H., Nekritz, E.A., Zeid, R., Gustafson, W.C., Greninger, P., et al. (2013). Targeting MYCN in neuroblastoma by BET bromodomain inhibition. Cancer Discov. 3, 308–323.

11. Zimmerman, M.W., Liu, Y., He, S., Durbin, A.D., Abraham, B.J., Easton, J., Shao, Y., Xu, B., Zhu, S., Zhang, X., et al. (2018). MYC Drives a Subset of High-Risk Pediatric Neuroblastomas and Is Activated through Mechanisms Including Enhancer Hijacking and Focal Enhancer Amplification. Cancer Discov. 8, 320–335.

12. Stathis, A., Zucca, E., Bekradda, M., Gomez-Roca, C., Delord, J.P., de La Motte Rouge, T., Uro-Coste, E., de Braud, F., Pelosi, G., and French, C.A. (2016). Clinical Response of Carcinomas Harboring the BRD4-NUT Oncoprotein to the Targeted Bromodomain Inhibitor OTX015/MK-8628. Cancer Discov. 6, 492–500.

13. Lewin, J., Soria, J.C., Stathis, A., Delord, J.P., Peters, S., Awada, A., Aftimos, P.G., Bekradda, M., Rezai, K., Zeng, Z., et al. (2018). Phase Ib Trial With Birabresib, a Small-Molecule Inhibitor of Bromodomain and Extraterminal Proteins, in Patients With Selected Advanced Solid Tumors. J. Clin. Oncol. 36, 3007–3014.

14. Setten, R.L., Rossi, J.J., and Han, S.P. (2019). The current state and future directions of RNAi-based therapeutics. Nat. Rev. Drug Discov. 18, 421–446.

15. Anthiya, S., Griveau, A., Loussouarn, C., Baril, P., Garnett, M., Issartel, J.P., and Garcion, E. (2018). MicroRNA-Based Drugs for Brain Tumors. Trends Cancer 4, 222–238.

16. Tonouchi, E., Gen, Y., Muramatsu, T., Hiramoto, H., Tanimoto, K., Inoue, J., and Inazawa, J. (2018). miR-3140 suppresses tumor cell growth by targeting BRD4 via its coding sequence and downregulates the BRD4-NUT fusion oncoprotein. Sci. Rep. 8, 4482.

17. Takagawa, Y., Gen, Y., Muramatsu, T., Tanimoto, K., Inoue, J., Harada, H., and Inazawa, J. (2020). miR-1293, a Candidate for miRNA-Based Cancer Therapeutics, Simultaneously Targets BRD4 and the DNA Repair Pathway. Mol. Ther. 28, 1494–1505.

18. Molenaar, J.J., Ebus, M.E., Geerts, D., Koster, J., Lamers, F., Valentijn, L.J., Westerhout, E.M., Versteeg, R., and Caron, H.N. (2009). Inactivation of CDK2 is

synthetically lethal to MYCN over-expressing cancer cells. Proc. Natl. Acad. Sci. USA *106*, 12968–12973.

19. Jakacki, R.I., Hamilton, M., Gilbertson, R.J., Blaney, S.M., Tersak, J., Krailo, M.D., Ingle, A.M., Voss, S.D., Dancey, J.E., and Adamson, P.C. (2008). Pediatric phase I and pharmacokinetic study of erlotinib followed by the combination of erlotinib and temozolomide: a Children's Oncology Group Phase I Consortium Study. J. Clin. Oncol. *26*, 4921–4927.

20. Keller, J., Nimnual, A.S., Varghese, M.S., VanHeyst, K.A., Hayman, M.J., and Chan, E.L. (2016). A Novel EGFR Extracellular Domain Mutant, EGFRΔ768, Possesses Distinct Biological and Biochemical Properties in Neuroblastoma. Mol. Cancer Res. *14*, 740–752.

21. Delmore, J.E., Issa, G.C., Lemieux, M.E., Rahl, P.B., Shi, J., Jacobs, H.M., Kastritis, E., Gilpatrick, T., Paranal, R.M., Qi, J., et al. (2011). BET bromodomain inhibition as a therapeutic strategy to target c-Myc. Cell *146*, 904–917.

22. Marshall, G.M., Liu, P.Y., Gherardi, S., Scarlett, C.J., Bedalov, A., Xu, N., Iraci, N., Valli, E., Ling, D., Thomas, W., et al. (2011). SIRT1 promotes N-Myc oncogenesis through a positive feedback loop involving the effects of MKP3 and ERK on N-Myc protein stability. PLoS Genet. *7*, e1002135.

23. Adhikary, S., and Eilers, M. (2005). Transcriptional regulation and transformation by Myc proteins. Nat. Rev. Mol. Cell Biol. *6*, 635–645.

24. Schafer, J.M., Lehmann, B.D., Gonzalez-Ericsson, P.I., Marshall, C.B., Beeler, J.S., Redman, L.N., Jin, H., Sanchez, V., Stubbs, M.C., Scherle, P., et al. (2020). Targeting MYCN-expressing triple-negative breast cancer with BET and MEK inhibitors. Sci. Transl. Med. *12*, eaaw8275.

25. Pugh, T.J., Morozova, O., Attiyeh, E.F., Asgharzadeh, S., Wei, J.S., Auclair, D., Carter, S.L., Cibulskis, K., Hanna, M., Kiezun, A., et al. (2013). The genetic landscape of high-risk neuroblastoma. Nat. Genet. *45*, 279–284.

26. Iniguez, A.B., Alexe, G., Wang, E.J., Roti, G., Patel, S., Chen, L., Kitara, S., Conway, A., Robichaud, A.L., Stolte, B., et al. (2018). Resistance to Epigenetic-Targeted Therapy Engenders Tumor Cell Vulnerabilities Associated with Enhancer Remodeling. Cancer Cell *34*, 922–938.e7.

27. Fong, C.Y., Gilan, O., Lam, E.Y.N., Rubin, A.F., Ftouni, S., Tyler, D., Stanley, K., Sinha, D., Yeh, P., Morison, J., et al. (2015). BET inhibitor resistance emerges from leukaemia stem cells. Nature *525*, 538–542.

28. Kurimchak, A.M., Shelton, C., Duncan, K.E., Johnson, K.J., Brown, J., O'Brien, S., Gabbasov, R., Fink, L.S., Li, Y., Lounsbury, N., et al. (2016). Resistance to BET Bromodomain Inhibitors Is Mediated by Kinome Reprogramming in Ovarian Cancer. Cell Rep. *16*, 1273–1286.

29. Shu, S., Lin, C.Y., He, H.H., Witwicki, R.M., Tabassum, D.P., Roberts, J.M., Janiszewska, M., Huh, S.J., Liang, Y., Ryan, J., et al. (2016). Response and resistance to BET bromodomain inhibitors in triple-negative breast cancer. Nature *529*, 413–417.

30. Ellinger-Ziegelbauer, H., Brown, K., Kelly, K., and Siebenlist, U. (1997). Direct activation of the stress-activated protein kinase (SAPK) and extracellular signal-regulated protein kinase (ERK) pathways by an inducible mitogen-activated protein Kinase/ERK kinase kinase 3 (MEKK) derivative. J. Biol. Chem. *272*, 2668–2674.

31. Lv, Y., Huang, Y., Xu, M., Heng, B.C., Yang, C., Cao, C., Hu, Z., Liu, W., Chi, X., Gao, M., et al. (2019). The miR-193a-3p-MAP3k3 Signaling Axis Regulates Substrate Topography-Induced Osteogenesis of Bone Marrow Stem Cells. Adv. Sci. (Weinh.) *7*, 1901412.

32. Channavajhala, P.L., Rao, V.R., Spaulding, V., Lin, L.L., and Zhang, Y.G. (2005). hKSR-2 inhibits MEKK3-activated MAP kinase and NF-kappaB pathways in inflammation. Biochem. Biophys. Res. Commun. *334*, 1214–1218.

33. Bonvin, C., Guillon, A., van Bemmelen, M.X., Gerwins, P., Johnson, G.L., and Widmann, C. (2002). Role of the amino-terminal domains of MEKKs in the activation of NF kappa B and MAPK pathways and in the regulation of cell proliferation and apoptosis. Cell. Signal. *14*, 123–131.

34. Sugiyama, H., Takahashi, K., Yamamoto, T., Iwasaki, M., Narita, M., Nakamura, M., Rand, T.A., Nakagawa, M., Watanabe, A., and Yamanaka, S. (2017). Nat1 promotes translation of specific proteins that induce differentiation of mouse embryonic stem cells. Proc. Natl. Acad. Sci. USA *114*, 340–345.

35. Fan, Y., Ge, N., Wang, X., Sun, W., Mao, R., Bu, W., Creighton, C.J., Zheng, P., Vasudevan, S., An, L., et al. (2014). Amplification and over-expression of MAP3K3 gene in human breast cancer promotes formation and survival of breast cancer cells. J. Pathol. *232*, 75–86.

36. Umapathy, G., El Wakil, A., Witek, B., Chesler, L., Danielson, L., Deng, X., Gray, N.S., Johansson, M., Kvarnbrink, S., Ruuth, K., et al. (2014). The kinase ALK stimulates the kinase ERK5 to promote the expression of the oncogene MYCN in neuroblastoma. Sci. Signal. *7*, ra102.

37. Sugimoto, T., Tatsumi, E., Kemshead, J.T., Helson, L., Green, A.A., and Minowada, J. (1984). Determination of cell surface membrane antigens common to both human neuroblastoma and leukemia-lymphoma cell lines by a panel of 38 monoclonal antibodies. J. Natl. Cancer Inst. *73*, 51–57.

38. Hino, T., Sugimoto, T., Matsumura, T., Horii, Y., Inazawa, J., and Sawada, T. (1989). Diverse responses to retinoid in morphological differentiation, tumorigenesis and N-myc expression in human neuroblastoma sublines. Int. J. Cancer *44*, 286–291.

39. Sugimoto, T., Gotoh, T., Yagyu, S., Kuroda, H., Iehara, T., Hosoi, H., Ohta, S., Ohira, M., and Nakagawara, A. (2013). A MYCN-amplified cell line derived from a long-term event-free survivor among our sixteen established neuroblastoma cell lines. Cancer Lett. *331*, 115–121.

40. Saito-Ohara, F., Imoto, I., Inoue, J., Hosoi, H., Nakagawara, A., Sugimoto, T., and Inazawa, J. (2003). PPM1D is a potential target for 17q gain in neuroblastoma. Cancer Res. *63*, 1876–1883.

41. Furuta, M., Kozaki, K., Tanimoto, K., Tanaka, S., Arii, S., Shimamura, T., Niida, A., Miyano, S., and Inazawa, J. (2013). The tumor-suppressive miR-497-195 cluster targets multiple cell-cycle regulators in hepatocellular carcinoma. PLoS ONE *8*, e60155.

42. Fujiwara, N., Inoue, J., Kawano, T., Tanimoto, K., Kozaki, K., and Inazawa, J. (2015). miR-634 Activates the Mitochondrial Apoptosis Pathway and Enhances Chemotherapy-Induced Cytotoxicity. Cancer Res. *75*, 3890–3901.

43. Gen, Y., Yasui, K., Kitaichi, T., Iwai, N., Terasaki, K., Dohi, O., Hashimoto, H., Fukui, H., Inada, Y., Fukui, A., et al. (2017). ASPP2 suppresses invasion and TGF-β1-induced epithelial-mesenchymal transition by inhibiting Smad7 degradation mediated by E3 ubiquitin ligase ITCH in gastric cancer. Cancer Lett. *398*, 52–61.

44. Gen, Y., Yasui, K., Zen, Y., Zen, K., Dohi, O., Endo, M., Tsuji, K., Wakabayashi, N., Itoh, Y., Naito, Y., et al. (2010). SOX2 identified as a target gene for the amplification at 3q26 that is frequently detected in esophageal squamous cell carcinoma. Cancer Genet. Cytogenet. *202*, 82–93.